# Interface Development and Encapsulation in Simultaneous Coinjection Molding of Disk. II. Two-Dimensional Simulation and Experiment

**C. T. Li, D. J. Lee, A. I. Isayev**

*Institute of Polymer Engineering, The University of Akron, Akron, Ohio 44325*

Received 14 March 2002; revised 22 July 2002; accepted 22 July 2002

**Abstract:** Two-dimensional simulation and experimental studies of flow-rate-controlled coinjection molding were carried out. Skin polymer was injected first, and then both skin and core polymers were injected simultaneously into a center-gated disk cavity through a two-channel nozzle to obtain an encapsulated sandwich structure. The physical modeling and simulation developed, reported in Part I of this series, were based on the Hele–Shaw approximation and the kinematics of the interface to describe the multilayer flow, and the interface development was used to predict the skin/core distribution in the moldings. The effects of rheological properties and processing conditions on the material distribution, penetration behavior, and breakthrough phenomena were investigated. The predicted and measured results were found to be in a good agreement. © 2003 Wiley Periodicals, Inc. J Appl Polym Sci 88: 2310–2318, 2003

**Key words:** coinjection molding; interface evolution; breakthrough; experiment; thermoplastics; simulation; rheology; encapsulation

## INTRODUCTION

The coinjection process was first introduced about 30 years ago.[1] Generally, the mechanics of this process relies on sequential injection of two materials through the same gate or gates or simultaneous injection of both skin and core materials after some amount of skin material is injected first into a cavity. Sometimes injection of a very additional small amount of the skin material will "cap" the end of the sequence described.

The coinjection molded parts, which have special characteristics, can be produced by the combination of two or more types of plastic materials, such as using the skin material to achieve required surface properties (e.g., appearance, hardness, thermal or chemical resistance, soft touch), while using the core material to obtain sufficient mechanical properties or to reduce cost (for example, using recycled materials). Selden[2] provided a good review of common technologies for the manufacture of coinjection molded products, material selection, and material combinations.

Coinjection molding requires advanced technical skills because many molding factors are involved. To understand the internal sandwich structure formation and the melt flow behavior in coinjection molding, it is important to design properly the coinjection-molding process. Only limited experimental studies on coinjection molding have been reported.[3–19] Most previous experimental investigations highlighted the importance of the role of the viscosity ratio between skin and core materials, as well as the rate of injection. Donovan et al.[3] were the first to carry out an experimental study of the two-shot injection-molding process. They applied the coinjection process to recycling thermoplastics. It appears that published reports of most early experimental studies on coinjection molding under various processing conditions and material combinations have been done by White et al.[4–7] They indicated that for isothermal conditions phase distribution is very sensitive to the viscosity ratio, which represents the primary influence of rheological properties on the interfacial shape in the sandwich-molded parts. In an isothermal sequential cavity filling of two melts, the most uniform skin–core structures occurred when the melt injected first possessed a slightly lower viscosity than the second one. Moreover, for simultaneous injection of two materials, in which two melts were injected into a mold in the form of an annular ring and a core, the melt with the lower viscosity did encapsulate the melt with the higher viscosity during the flow in the runner section, and a skin–core sandwich configuration resulted in the cavity. However, if the annulus contained a higher viscosity melt, phase inversion might occur. Later on, sequential coinjection molding of reinforced polymer under nonisothermal conditions was carried out by Akay[8] using a center-gated disc mold in order to investigate the type of skin–core structure, interface adhesion, and interface instability. He found that conditions for obtaining a

*Correspondence to:* A. I. Isayev (aisayev@uakron.edu).
Contract grant (fellowship) sponsor: Lord Corporation.

Journal of Applied Polymer Science, Vol. 88, 2310–2318 (2003)

certain type of skin–core structure under nonisothermal flow conditions were substantially different from the isothermal flow conditions used by White and coworkers.[4–7] The order of injection was not significant in obtaining a skin–core structure for reinforced polymer, but it was important in obtaining extensive phase interlocking. The latter was reduced if the flow rate and the mold temperature were low. Interface instability appeared to be more pronounced if the high viscosity melt occupied the skin and if the injection speed was high.

Kuhmann and Ehrenstein[9] performed monosandwich injection-molding experiments using a conductive, filled (45 wt %) poly(ether sulfone) (PES), as a skin material and unfilled PES as a core material. The injection rate was found to be the most important processing parameter influencing the core distribution. The filler distribution near the surface was hardly influenced. The resulting small viscosity ratios did not cause flow instabilities affecting the core distribution. Flow behavior during a sequential coinjection process using acrylonitrile-butadiene-styrene (ABS) polymer as a skin material and a core material that contained a black pigment for observation was investigated by Derdouri et al.[10] They varied the skin/core ratio, the mold and melt temperatures, the speed of injection, and the skin/core viscosity ratio. They found that, in addition to the viscosity ratio having an important effect on the onset of breakthrough, there is a critical skin/core ratio below which breakthrough occurs. Under the same conditions breakthrough is more sensitive to the mold temperature than to the melt temperature. The fingering instability resulting from the difference in viscosities of the two materials gave rise to early breakthrough of the core material and a nonuniform skin layer thickness.[11] The developing behavior of core material and breakthrough phenomenon in sandwich injection molding was also investigated by Watanabe et al.,[12] who used a spiral-flow mold, by changing the viscosity ratio and the melt temperature of skin and core materials. They concluded that the breakthrough phenomenon depended not only on the melt strength of the freezing layer of the skin material but also on the draw ratio of the skin material at the flow front.

Selden[13] employed the monosandwich injection technique to investigate experimentally the effects of processing conditions on material distribution and layer thickness in three dimensions and on mechanical properties such as flexural and impact strength. He showed that three parameters, namely, injection velocity, core temperature, and core content are the most significant process variables affecting skin/core distribution. A high core temperature is the most important variable for obtaining a constant core thickness, while the volume of injected core is the most significant factor leading to a breakthrough phenomenon.

Thus far, the study of simultaneous coinjection molding has received little attention. Somnuk and Smith[14] carried out an experimental study on the simultaneous coinjection-molding process. According to them the main advantage of this technique is the ability to control the coinjection process in a manner virtually identical to conventional single-phase injection molding if the length of the simultaneous phase is fixed. Lee et al.[15] performed simultaneous sandwich injection molding on an end-gated rectangular mold. They found that an additional advantage of the simultaneous coinjection technique is being able to utilize materials with a broader range of viscosity ratios. Eigl and Langecker[16] conducted simultaneous sandwich injection molding to determine empirically the interrelation of individual limiting quantities (important processing parameters and material properties) and the essential effects of the melt flow during the mold-filling process. Based on their experiments, they proposed a phenomenological approach to describe layer thickness formation and the spatial distribution of the components in the molded parts, with the purpose of constructing a simulation model that was close to practical operation. In addition, Kadota et al.[17] performed sequential coinjection molding of polystyrene/polypropylene to investigate the structure gradients as a function of the process history and injection sequence. The skin–core–skin sequential coinjection-molding process was also used as a method for visualization by Chen et al.[18,19] to investigate polymer melt flow behavior and the fountain flow effect.

In the present study a physical model and process simulation of coinjection molding, previously developed as reported on in previous Part I of this series[20] and based on the kinematics and dynamics of interface evolution, combined with a Hele–Shaw approximation, was used to predict interface development in the simultaneous coinjection of both skin and core polymers in a flow-rate control process with acertain amount of skin polymer injected first. An experimental study was performed on a center-gated disk cavity to verify the simulation results. The effect of material properties and processing parameters on the interface distribution also was evaluated, such that the simultaneous flow-rate control coinjection-molding process could be optimized.

## EXPERIMENTAL

### Materials and their characterization

The materials used in the experiments included four polymers: low-density polyethylene (LDPE 640M), high-density polyethylene (HDPE 30360M), and two grades of polystyrene (PS 615APR and PS 623). These commercial thermoplastics were supplied by Dow Chemical Company (Midland, MI). They are listed in Table I.

**TABLE I**
**Characteristics of Materials[22]**

| Designation | Source grade | Zero shear viscosity at 180°C [Pa · s]* |
|---|---|---|
| PS 615 | Dow Chemical Co.STYRON 615 APR | $12.34 \times 10^3$ |
| LDPE | Dow Chemical Co. 640M | $9.516 \times 10^3$ |
| HDPE | Dow Chemical Co. 30360M | $0.489 \times 10^3$ |
| PS 623 | Dow Chemical Co. STYRON 623 | $37.17 \times 10^3$ |

* Zero shear viscosity at 180°C was obtained from extrapolated experimental data.

To carry out the study, it was necessary to choose material pairs based on their rheological properties. In Table II the material combinations used in these experiments are summarized. Here and throughout this article the core material is written first. The shear viscosity ratios at zero shear rate and at $\gamma = 10^2\ s^{-1}$ are also given.

The thermal properties of various materials used in this study were assumed to be constant and independent of temperature. The density of polymer melt during the filling stage was also taken to be constant. These properties of the polymers are listed in Table III.

Rheological characterization of these four thermoplastics (LDPE, HDPE, PS 615, and PS 623) was performed at temperatures of 160°C, 180°C, 200°C, and 220°C over a wide range of shear rates using a Rheometrics Mechanical Spectrometer (Model RMS-800) in the cone-and-plate mode within a low shear-rate region and an Instron Capillary Rheometer (Model 3211) in a high shear-rate region. The viscosity data were plotted as a function of shear rate at different temperatures, as shown in Figures 1–3, and then fitted to the modified four-parameter Cross model[21] to determine the model constants, $A$, $T_b$, $\tau^*$, and $n$, that were required in process simulation. Table IV lists all these parameters.

**TABLE II**
**Material Combinations[22]**

| System (core/skin) | Zero shear viscosity ratio ($R^*$) | Viscosity ratio at $\dot{\gamma} = 10^2\ s^{-1}$ |
|---|---|---|
| HDPE/PS 615 | 0.04 | 0.15 |
| HDPE/LDPE | 0.05 | 0.23 |
| LDPE/PS 615 | 0.77 | 0.64 |
| PS 615/LDPE | 1.30 | 1.56 |
| LDPE/HDPE | 19.46 | 4.37 |
| PS 615/HDPE | 25.24 | 6.80 |
| PS 623/LDPE | 3.91 | 2.31 |
| LDPE/PS 623 | 0.26 | 0.43 |

*$R = \eta_{core}/\eta_{skin}$.

**TABLE III**
**Physical Properties of Polymers[22]**

| Properties | PS | LDPE | HDPE |
|---|---|---|---|
| $\rho^o \times 10^3$ (kg/m$^3$) | 1.04 | 0.921 | 0.960 |
| $\rho \times 10^3$ (kg/m$^3$) | 0.984 | 0.771 | 0.821 |
| $C_p$ (J/kg K) | 1420 | 2079 | 3500 |
| K (W/m K) | 0.17 | 0.30 | 0.48 |

$\rho^o$ at $T = 25$°C and $\rho$ at $T = 180$°C.

## Coinjection-molding experiment and interface measurements

The sandwich injection-molding apparatus consisted of two ram-type mini-injection-molding machines, which were connected in parallel to each other by a specially designed connector with a two-channel nozzle, and a visualized mold assembly. One of the machines was a Morgan Press (Model G-55), used to inject the core material, which flowed through the central nozzle (inner channel). The other was a Newbury Mini Molder (Model 45 Mini-Jector), used to inject the skin material, which flowed through the ring nozzle (outer channel). Both machines were vertical-type injection units with a mechanical clamping system actuated by compressed-air pressure. One of the polymer melts was colored for better visualization. A schematic drawing of sandwich injection-molding apparatus used in this study is shown in Figure 4. The sandwich injection-molding experiments[22] were conducted under various processing conditions. Table V lists the various processing parameters used in this study. Experiments and simulations were performed for Runs 1, 2, 4, 5, 6, and 13–15. In addition, simulations were carried out for all the other runs.

Center-gated disc specimens, 25.4 mm in diameter and 4.0 mm in thickness, were used (Fig. 5). To obtain an encapsulated skin/core structure using a simultaneous coinjection-molding process, it was necessary to

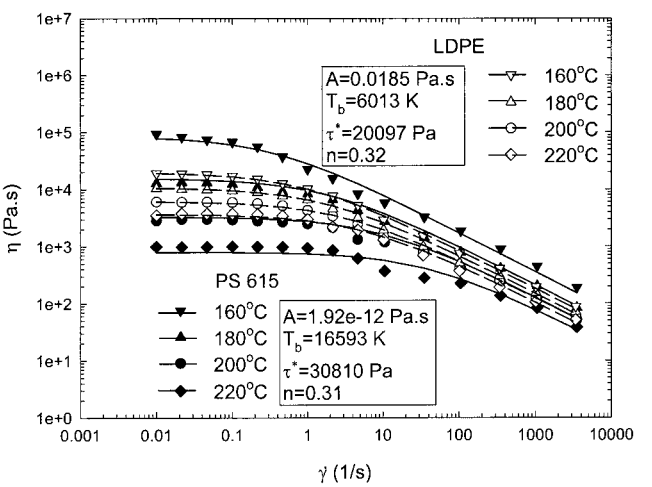


**Figure 1** Measured (symbols) and fitted (curves) viscosity of PS 615A and LDPE 640M as a function of shear rate.

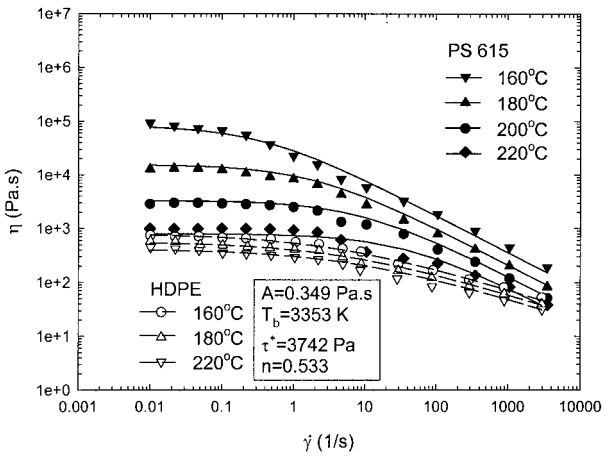


**Figure 2** Measured (symbols) and fitted (curves) viscosity of PS 615A and HDPE 30360M as a function of shear rate.

inject a certain amount of skin melt first, before the simultaneous phase of injection of the skin and core melts. In this study about 40 vol % of intended skin melt was injected first at a flow rate of 20 $cm^3/s$. The mold temperature was 80°C. To characterize the interface distribution of the two polymers, the molded parts were cut with a fresh razor in at least six positions, equally divided from the gate to the end of cavity. The gapwise interface distribution along the flow direction was measured using a microscope and described in terms of dimensionless thickness with respect to the streamwise direction. The obtained data will be compared with the simulated results.

## RESULTS AND DISCUSSION

### Effect of material properties

Phase distribution is very sensitive to the viscosity ratio. As indicated by White et al.,[4–7] the viscosity ratio represents the dominant factor influencing the

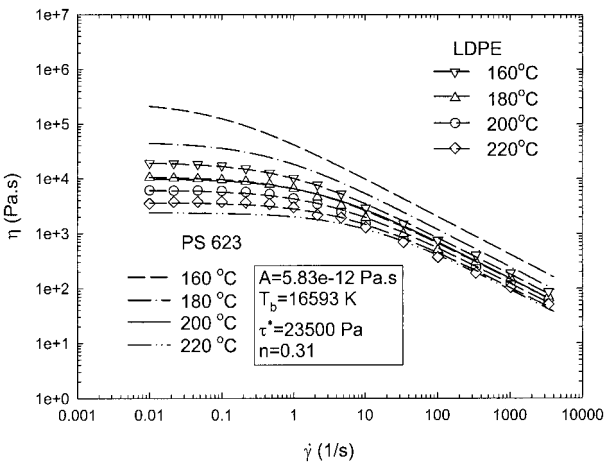


**Figure 3** Measured (symbols) and fitted (curves) viscosity of PS 623 and LDPE 640M as a function of shear rate.

**TABLE IV**
**Parameters of Cross Model**

| Materials | A (Pa · s) | $T_b$ (k) | $\tau^*$ (Pa) | $n$ |
|---|---|---|---|---|
| PS 615 | 1.92e-12 | 16593 | 30810 | 0.31 |
| PS 623 | 5.83e-12 | 16593 | 23500 | 0.31 |
| LDPE | 0.0185 | 6013 | 20097 | 0.32 |
| HDPE | 0.3491 | 3353 | 3742 | 0.533 |

interface shape during an isothermal cavity filling. They found that if two melts were injected into a mold in the form of an annular ring and a core, the configuration of the interface was stable only if the annulus contained a low viscosity melt. If the annulus contained a higher viscosity melt, a phase inversion might occur. Figure 6(a) shows numerical and experimental interface shape for coinjection molding of material pairs PS 615 and LDPE at the end of a cavity filling. Open symbols represent the experimental data, and solid symbols are the simulated results. The corresponding measured and fitted flow curves of both the PS 615 and LDPE materials are presented in Figure 1. Cross model is used for the fitting. Note that, as shown in Figure 6(a), when the high-viscosity polymer, PS 615, was injected as a core component, the thickness of the core phase increased correspondingly. Also, less penetration of the core melt into the skin melt along the streamwise direction was observed at the end of cavity filling. These effects resulted from the high-viscosity core melt displacing the low-viscosity skin melt in order to release pressure acting on the core layer. Figure 6(b) shows the numerical and experimental interface shape for coinjection molding of the material combination of PS 615 and HDPE. Here HDPE has a much lower viscosity than PS 615, which can clearly be seen in the measured and fitted flow curves shown in Figure 2. Both the measurement and simulation shown in Figure 6(b) indicate that when a much lower viscosity material was injected as the core component, it normally led to the breakthrough phenom-

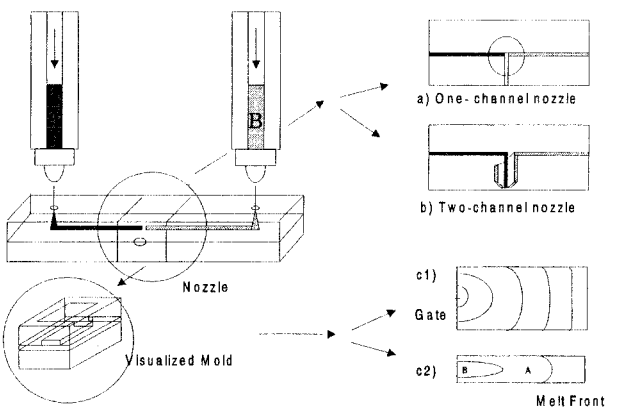


**Figure 4** Schematic diagram of coinjection-molding apparatus.[22]

**TABLE V**
**Processing Conditions for Simultaneous Coinjection-Molding Experiments and Simulations**

| Run No. | Material combination core (C)/skin (S) | Viscosity ratio ($\eta_c/\eta_s$) | Flow rate ratio ($Q_c/Q_s$) | Melt temperature core/skin (°C/°C) | Mold temperature (°C) | Volume of first injected skin melt |
|---|---|---|---|---|---|---|
| 1 | PS 615/LDPE | 1.3 | 1.5 | 180/180 | 80 | 40% |
| 2 | LDPE/PS 615 | 0.77 | 1.5 | 180/180 | 80 | 40% |
| 3 | PS 615/HDPE | 25.24 | 1.5 | 180/180 | 80 | 40% |
| 4 | HDPE/PS 615 | 0.04 | 1.5 | 180/180 | 80 | 40% |
| 5 | PS 623/LDPE | 3.91 | 1.8 | 180/180 | 80 | 40% |
| 6 | LDPE/PS 623 | 0.26 | 1 | 180/180 | 80 | 40% |
| 7 | PS 615/LDPE | 1.3 | 5.0 | 180/180 | 80 | 40% |
| 8 | PS 615/LDPE | 1.3 | 3.0 | 180/180 | 80 | 40% |
| 9 | PS 615/LDPE | 1.3 | 2.0 | 180/180 | 80 | 40% |
| 10 | PS 615/LDPE | 1.3 | 1.0 | 180/180 | 80 | 40% |
| 11 | PS 615/LDPE | 1.3 | 0.5 | 180/180 | 80 | 40% |
| 12 | PS 615/LDPE | 1.3 | 0.2 | 180/180 | 80 | 40% |
| 13 | PS 615/LDPE | 1.3 | 1.8 | 160/160 | 80 | 40% |
| 14 | PS 615/LDPE | 1.3 | 1.5 | 180/180 | 80 | 40% |
| 15 | PS 615/LDPE | 1.3 | 1.5 | 220/220 | 80 | 40% |
| 16 | PS 615/LDPE | 1.3 | 1 | 160/180 | 80 | 40% |
| 17 | PS 615/LDPE | 1.3 | 1 | 180/180 | 80 | 40% |
| 18 | PS 615/LDPE | 1.3 | 1 | 220/180 | 80 | 40% |
| 19 | PS 615/LDPE | 1.3 | 1 | 180/160 | 80 | 40% |
| 20 | PS 615/LDPE | 1.3 | 1 | 180/180 | 80 | 40% |
| 21 | PS 615/LDPE | 1.3 | 1 | 180/220 | 80 | 40% |
| 22 | PS 615/LDPE | 1.3 | 1 (20:20) | 180/180 | 80 | 40% |
| 23 | PS 615/LDPE | 1.3 | 1 (40:40) | 180/180 | 80 | 40% |
| 24 | PS 615/LDPE | 1.3 | 1 (60:60) | 180/180 | 80 | 40% |
| 25 | PS 615/LDPE | 1.3 | 1 (100:100) | 180/180 | 80 | 40% |
| 26 | PS 615/LDPE | 1.3 | 1 | 180/180 | 80 | 20% |
| 27 | PS 615/LDPE | 1.3 | 1 | 180/180 | 80 | 30% |
| 28 | PS 615/LDPE | 1.3 | 1 | 180/180 | 80 | 40% |
| 29 | PS 615/LDPE | 1.3 | 1 | 180/180 | 80 | 60% |
| 30 | PS 615/LDPE | 1.3 | 1 | 180/180 | 80 | 80% |

enon. Furthermore, the less viscous core-melt layer also showed a reduction of the core thickness during the cavity filling. Consequently, the less viscous core melt flows faster to the end of then cavity than higher viscous skin melt, resulting in the breakthrough of the core polymer at the skin melt front.

Figure 7 shows the simulated and measured interface shape for coinjection molding of another pair, PS 623 and LDPE, at the end of cavity filling. PS 623 had a higher zero shear-rate viscosity than did PS 615. The measured and fitted shear viscosity functions of PS 623 and LDPE are given in Figure 3. It can be seen in Figure 7 that the observed behavior is similar to that shown in Figure 6. Note that there is very good agreement between the results of the numerical simulations and the measurements.

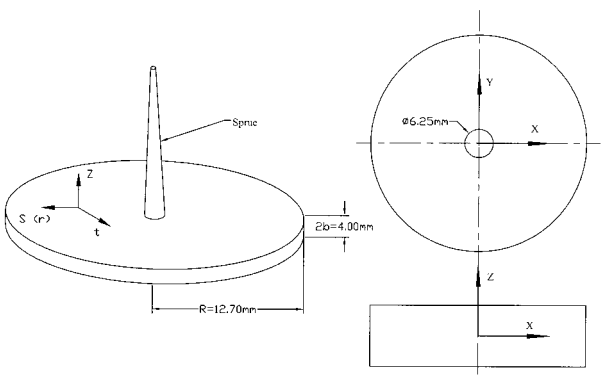


**Figure 5** The coordinate system and dimensions of the center-gated disk cavity.

Figure 8 shows the calculated pressure distributions along the flow direction at the end of cavity filling for different material combinations. It indicates that the higher the viscosity of the skin polymer, the higher the pressure gradient. Thus, the material pair LDPE/PS 623 required the highest pressure gradient, whereas the pair PS 615/HDPE needed the lowest.

Figure 9 shows the calculated gapwise temperature distribution at the end of cavity filling for several material combinations for the cross section at $r = 0.748$ cm from the entrance. It can be seen that near the wall the material pairs LDPE/PS and HDPE/PS have higher temperatures than do the pairs PS/LDPE and PS/HDPE. This is because of the higher shear-rate region—the higher viscosity of the skin component of the LDPE/PS and HDPE/PS pairs causes the higher heat dissipation.

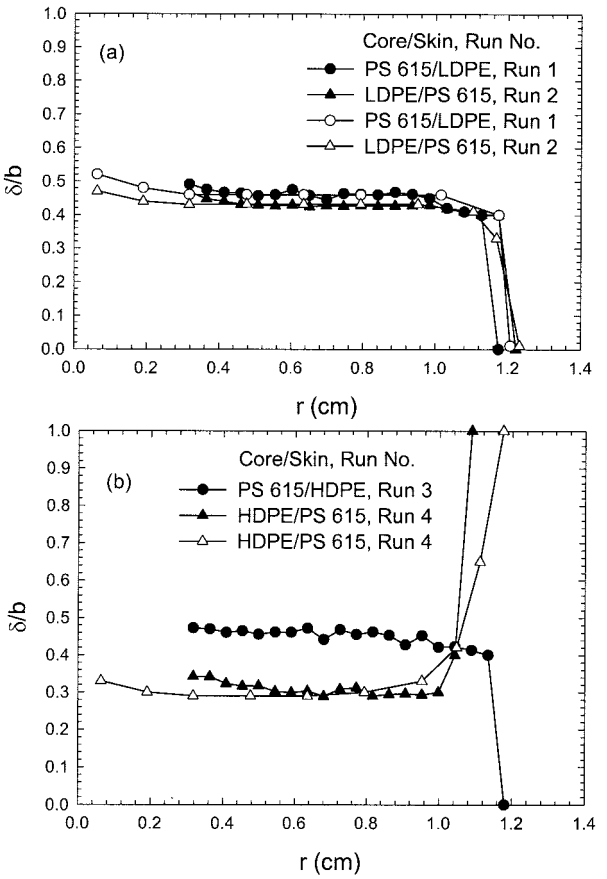


**Figure 6** Measured (open symbols) and calculated (filled symbols) interface distribution in coinjection moldings obtained at a melt temperature of 180°C and a flow rate ratio of 1.5.

In the present study the zero-shear-rate viscosity ratio varied from 0.04 to 25.24. It was concluded that increasing the viscosity of the core melt resulted in a lower penetration and a thicker layer of the core. In contrast, a decrease of the viscosity of the core melt or an increase of the viscosity of the skin melt led to the breakthrough phenomenon. Compared with the skin in sequential coinjection molding,[13,22,23] the skin in simultaneous coinjection molding is more uniform. Furthermore, our experimental and simulated data indicated that an advantage of the simultaneous coinjection-molding process is that materials with a broader viscosity range can be utilized, a finding in agreement with experimental observations of Somnuk and Smith.[14]

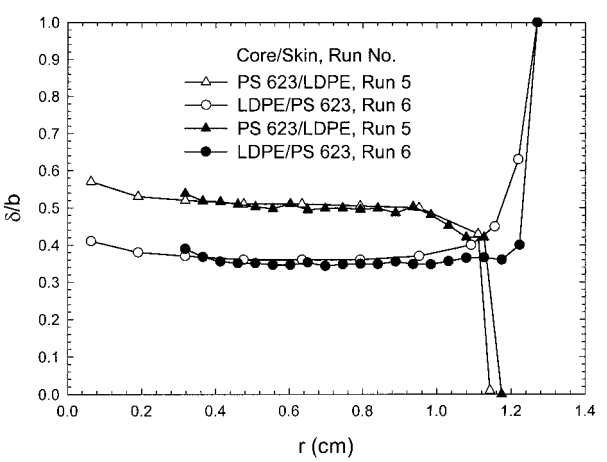


**Figure 7** Measured (open symbols) and calculated (filled symbols) interface distribution in coinjection moldings obtained at a melt temperature of 180°C and a flow rate ratio for PS/LDPE of 1.8, for LDPE/PS of 1.

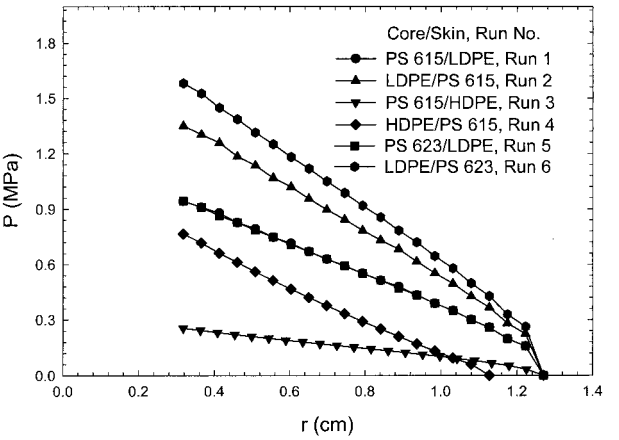


**Figure 8** Pressure distribution along the flow direction at the end of cavity filling.

## Effect of melt temperature

The effect of melt temperature on the interface distribution under nonisothermal flow conditions is quite complex because increasing the melt temperature decreases the viscosity of both the skin and core melts. However, the magnitude of the effect depends on the

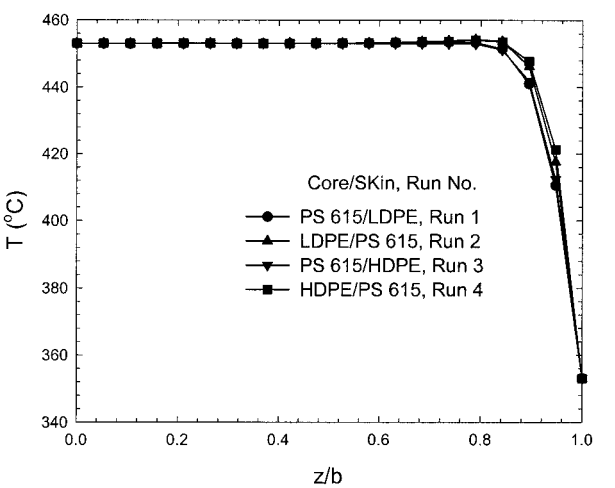


**Figure 9** Gapwise temperature distribution at the end of cavity filling for the cross section at $r = 0.746$ cm from the entrance.

individual polymer components and the activation energies of the viscous flow.

Figure 10 shows the experimental and simulated results of the effect of both core (PS 615) and skin (LDPE) melt temperatures on the interface shape at the end of cavity filling. It can be seen that increasing the melt temperature of both polymers led to a slight decrease in the thickness of the core melt. Increasing the melt temperature induced a larger decrease in the viscosity of the core melt (PS 615) than in the skin melt (LDPE). This is because the temperature sensitivity of the viscosity of PS 615 ($T_b$ = 16,593 K) was higher than that of LDPE ($T_b$ = 6013 K), as shown in Figure 1 and Table II. From Figure 10 it is also evident that the interface thickness was affected by the change in the flow rate ratio (Run 13) in addition to the melt temperature.

The effect of the melt temperature variation on the interface distribution can be observed further in Figure 11(a,b), in which the results of simulation are shown for the cases where variation in melt temperature was for the skin or core only. It can be seen from Figure 11(b) that when only skin melt temperature variation took place, core melt thickness was maintained, remaining the same at all three temperatures. Only a slight decrease of the penetration length was observed with the higher melt temperature of the skin. Figure 11(a) shows that the effect of varying the core melt temperature on the interface distribution was more significant. Namely, there was a slight reduction of the core thickness because of the increase in the core melt temperature. Thus, the effect of the core temperature was more appreciable as a result of the high temperature sensitivity of the viscosity of the core polymer melt, PS 615.

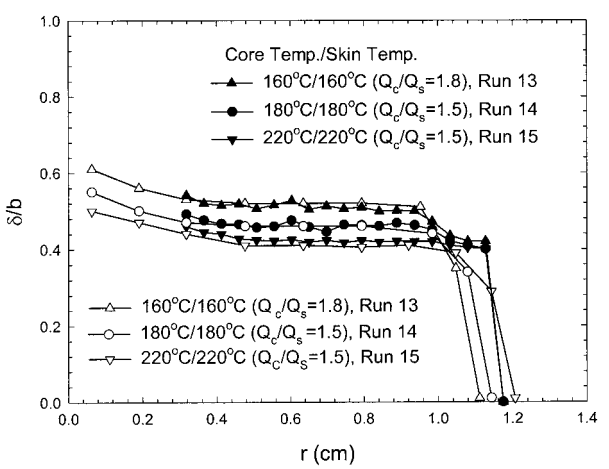


**Figure 10** Measured (open symbols) and calculated (filled symbols) gapwise interface distributions in coinjection moldings of PS 615/LDPE at various melt temperatures.

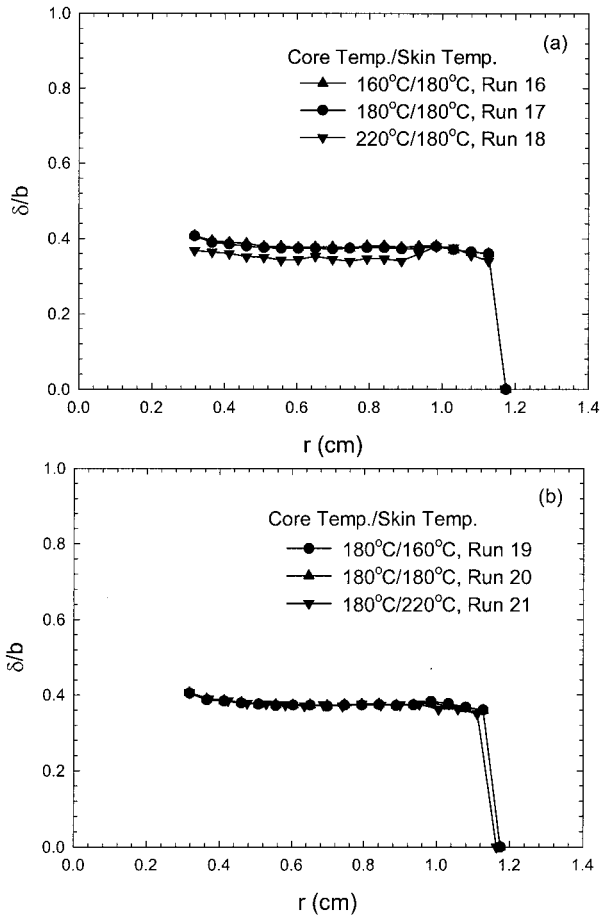


**Figure 11** Calculated gapwise interface distributions in coinjection moldings of PS 615/LDPE obtained at a flow rate ratio of 1 and at various (a) core and (b) skin melt temperatures.

## Effect of injection speed (flow rate)

In simultaneous coinjection molding, the injection rate ratio of the two polymer melts strongly affects the skin/core distribution of moldings because of a strong dynamic interaction of both polymer melts at the interface. Figure 12 shows the effect of core:skin flow rate ratio on the calculated gapwise interface distribution at the end of cavity filling of PS 615/LDPE. The melt temperatures of both the skin and core were maintained at 180°C, indicating that an increase in the flow rate ratio led to a significant increase in the thickness of the core melt phase. Meanwhile, the length of penetration of the core melt into the skin melt decreased because the higher the injection rate, the higher the pressure. When the core melt had a higher injection rate, in addition to being able to push slightly more skin melt in the flow direction, it also could push significantly more in the thickness direction. The shear rate is much higher near the mold wall than that at the center region; thus, shear-thinning behavior is more pronounced near the wall region, resulting in a much lower viscosity for the skin poly-

mer at a higher flow rate ratio. Both effects imply that the higher thickness fraction of the core component and the corresponding lesser penetration along the flow direction result from a higher injection speed ratio.

Figure 13(a) shows that the effect of flow rate at a constant flow rate ratio of 1 on the calculated interface distribution at the end of cavity filling for the material combination PS 615/LDPE. The melt temperatures of both components are the same: $T_m$ = 180°C, $T_w$ = 80°C. It was found that even though flow rate increased a lot, the thickness of the core melt layer remained almost the same. This is because both skin and core melt flow rates increased at the same ratio, with both components experience increasing high pressure at the same time. Thus, their interaction did not lead to a change in interface shape.

The present calculation also showed that the effect of the injection rate ratio on the interface evolution was significantly larger than that of the melt temperature and the viscosity ratio. This is evident from comparison of the results in Figures 10 and 12. Also, as shown in the present study, in simultaneous coinjection molding the effect of the injection ratio on interface thickness was more evident than that in the sequential coinjection molding, as shown by Schlatter et al.[23] Significantly, the breakthrough phenomenon can even be eliminated by adjusting the injection rate of the core melt, as shown by the calculations presented in this study and by the experimental observations of Somnuk and Smith.[14] This is because the injection rates of the skin and core melts are in effect controlled independent of each other.

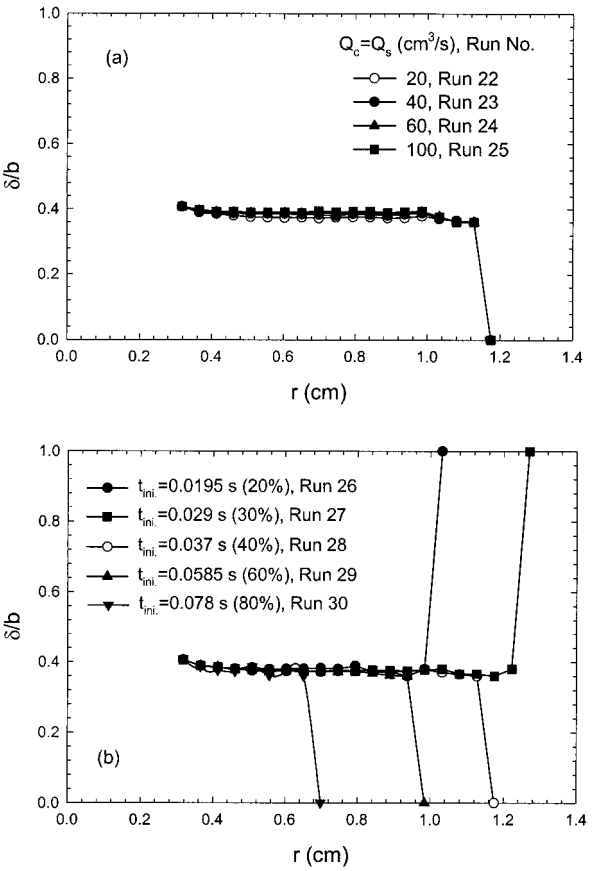


**Figure 13** Calculated gapwise interface distributions in coinjection moldings of PS 615/LDPE obtained at a melt temperature of 180°C and at various (a) flow rates and (b) durations of simultaneous injection phase.

### Effect of duration of simultaneous injection

To obtain optimum skin/core sandwich structure in molded parts made by simultaneous coinjection molding, a major task is to find the proper time interval between the injection of a certain amount of skin polymer (single phase) and the following simultaneous injection of both polymers (simultaneous phase). The proper stroke and the duration of the simultaneous phase depend on the material pairs and the mold geometry. In the experiments and in the simulation it was observed that encapsulation was always possible for simultaneous injection of two polymer melts having a viscosity ratio (core/skin) greater than 1 when a certain amount of the intended core melt was injected first before the simultaneous injection of the intended skin and core melts.

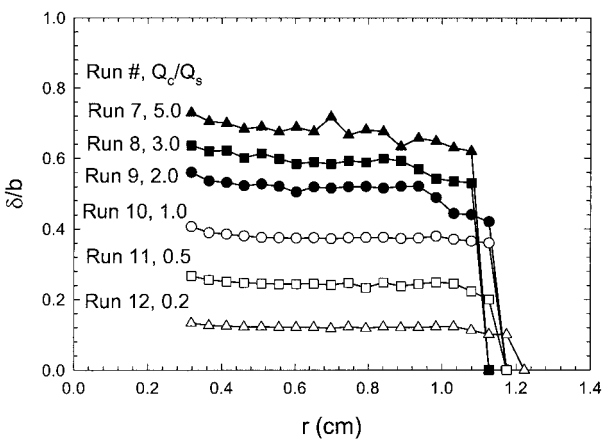


**Figure 12** Calculated gapwise interface distributions in coinjection moldings of PS 615/LDPE obtained at a melt temperature of 180°C and at various flow rate ratios.

Figure 13(b) shows the effect of the duration of the simultaneous phase on the interface distribution at the end of filling of PS 615/LDPE. The melt temperature ($T_m$) is 180°C, and the injection rate for both skin and core melts is 20 $cm^3$/s. It was found that when the time interval of the initial single-phase injection was too short, the core melt penetrated the skin melts, resulting in breakthrough, which would lead to discarding of the moldings. If the time interval were too long, it resulted in less penetration along the flow

direction and left a large amount of the skin melt in the far-end region of the cavity. It was also noted that the duration of the simultaneous injection phase of the specific polymer pairs significantly affected the length of penetration in the flow direction but did not affect the core layer thickness. In other words, the thickness of the core melt phase was independent of the injection stroke and the duration of the simultaneous phase.

## CONCLUSIONS

Numerical and experimental studies of a two-dimensional nonisothermal transient two-phase flow in the simultaneous coinjection-molding process were performed. Both simulated and measured results indicate that to obtain the optimum encapsulated skin/core structure in simultaneous coinjection–molded parts, it is necessary to select proper material combinations and processing parameters. The results have shown that material pairs with a broad range of viscosities may be utilized in this process. For a specific material combination, the injection rate ratio had the strongest effect on the interface position and the thickness of the core melt phase. The duration of simultaneous injection had a significant effect on the penetration length of a core melt into a skin melt in the streamwise direction. However, the variation in melt temperature shows that there was only a slight effect on the interface evolution. The breakthrough phenomenon was determined mainly by the volume of the initially injected single-phase melt and the rheological properties of the material combination.

## References

1. Garner, P. J.; Oxley, D. F. Brit. Pat. 1,156,217 (1969).
2. Selden, R. J Inj Mold Technol 1997, 1, 189.
3. Donovan, R. C.; Rabe, K. S.; Mammel, W. K.; Lord, H. A. Polym Eng Sci 1975, 15, 774.
4. White, J. L.; Lee, B. L. Polym Eng Sci 1975, 15, 481.
5. Young, S. S.; White, J. L.; Clark, E. S.; Y. Polym Eng Sci 1980, 20, 798.
6. White, J. L.; Dee, H. B. Polym Eng Sci 1974, 14, 212.
7. Young, S. S.; White, J. L.; Clark, E. S.; Oyanagi, Y. SPE ANTEC 1980, 26, 163.
8. Akay, G. Polym Comp 1983, 4, 256.
9. Kuhmann, K.; Ehrenstein, G. W. SPE ANTEC 1998, 44, 372.
10. Derdouri, A.; Garcia-Rejon, A.; Nguyen, K. T.; Simard, Y.; Koppi, K. A.; Salamon, B. A. SPE ANTEC 1999, 45, 481.
11. Nguyen, K. T.; Turcott, E.; Derdouri, A.; Ait Messaoud, D.; Sanschagrin, B.; Salamon, B. A.; Koppi, K. A. SPE ANTEC 2000, 46, 533.
12. Watanabe, D.; Hamada, H.; Tomari, K. SPE ANTEC 2001, 47, 656.
13. Selden, R. Polym Eng Sci 2000, 40, 1165.
14. Somnuk, P.; Smith, G. F. SPE ANTEC 1995, 41, 760.
15. Lee, D. J.; Isayev, A. I.; White, J. L. SPE ANTEC 1998, 44, 346.
16. Eigl, F. A.; Langecker, G. R. SPE ANTEC 1997, 43, 456.
17. Kadota, M.; Cakmak, M.; Hamada, H. Polymer 1999, 40, 3119.
18. Chen, S. C.; Hsu, K. F.; Huang, J. S. Int Comm Heat Mass Trans 1994, 21, 499.
19. Chen, S. C.; Hsu, K. F.; Jung, W. R. SPE ANTEC 1994, 40, 671.
20. Li, C. T.; Isayev, A. I. J Appl Polym Sci 2003, 88, 2300.
21. Isayev, A. I., Ed. Injection and Compression Modeling Fundamentals; Marcel Dekker: New York, 1987.
22. Lee, D. J. Ph.D. Dissertation, University of Akron, 1998.
23. Schlatter, G.; Davidoff, A.; Agassant, J. F.; Vincent, M. SPE ANTEC 1995, 43, 456.